

Real-Time 3D Color Flow Doppler for Guidance of Vibrating Interventional Devices

MATTHEW P. FRONHEISER,¹ PATRICK D. WOLF,¹ SALIM F. IDRISSE,² RENDON C. NELSON,³
WARREN LEE⁴ AND STEPHEN W. SMITH¹

¹*Department of Biomedical Engineering
Duke University
Durham, NC 27708
mpf3@duke.edu*

²*Department of Pediatric Cardiology
Duke University Medical Center
Durham, NC 27710*

³*Department of Radiology
Duke University Medical Center
Durham, NC 27710*

⁴*GE Global Research
Niskayuna, NY 12309*

The goal of this investigation was to examine the feasibility of guiding interventional devices using piezoelectric buzzers to create velocity sources, which were imaged and tracked with real-time 3D color flow Doppler. The interventional devices examined in this study included a pacemaker lead, Brockenbrough needle for cardiac septal puncture, cardiac guidewire and radiofrequency ablation needles for cancer therapy. Each was mechanically coupled to a piezoelectric buzzer and was imaged using a commercial real-time 3D ultrasound system with either a 2.5 MHz matrix array transducer or a 5 MHz, 22 F catheter transducer equipped with a tool port. *In vitro* images acquired in tissue phantoms, excised liver with a 'tumor' target and an excised sheep heart show strong vibration signals in 3D color flow Doppler, enabling real-time tracking and guidance of all the devices in three dimensions. In a sheep model, *in vivo* tracking of the pacing lead was performed in the superior vena cava as well as the right atrium using RT3D color flow Doppler images. The vibrating rf ablation needles were guided through the liver toward "tumor" targets *in vivo* with real-time 3D color flow Doppler images.

Key words: V, , Color flow Doppler; device guidance; two-dimensional array; volumetric imaging.

I. INTRODUCTION

Cardiac pacemaker leads are commonly implanted under guidance of single plane fluoroscopy. In this sense, it is similar to other minimally-invasive interventional procedures such as percutaneous catheterization and needle pericardiocentesis. In each of these procedures, the pacemaker lead, the catheter and the needle show high x-ray image contrast. However, fluoroscopic guidance suffers from poor soft tissue contrast, lack of depth information and the risks of ionizing radiation to both patient and health care staff.

Other interventional procedures, such as treatment of liver tumors, are guided using computed tomography (CT) combined with fluoroscopy to overcome the tissue contrast and depth limitations. However, the patients are exposed to a larger radiation dose and such procedures require a dedicated CT system. These limitations have led to investigations of alternate methods of catheter and needle guidance using ultrasound imaging.

Armstrong et al¹ used an FDA-approved commercial device, the ColorMark (Echocath, Princeton, NJ) to couple kHz vibrations into an aspiration needle. These vibrations were detected and displayed with the color Doppler feature of a B-scan system in a clinical trial applied to pericardiocentesis. The needle tip is at a vibration anti-node with motion $x = A \sin(\omega t)$ and tip velocity $v = dx/dt = \omega A \cos(\omega t)$, where A is the amplitude for the vibration frequency (f). The tip velocities are detected and localized with color flow Doppler. The vibration of the needle tip acts as a strong velocity source with a typical peak amplitude of 15 mm and typical velocity range of 9-28 cm/s. The *in vitro* measurements described by this group showed good location accuracy over a range of needle depths up to 180 mm in an ultrasound phantom. Accuracy of needle location did not correlate with needle angle, needle length, needle depth in the phantom or mechanical constraints on the needle hub. One could foresee that such a technique for real-time detection and guidance could be applied in guiding other minimally invasive devices. However, it is also noteworthy that the authors recognized the limitation of ‘the 2-dimensional planar nature of the ultrasound beam.’

Others have examined the use of 3D ultrasound to overcome the limitations of 2D ultrasound in guiding interventional devices during liver tumor treatment. Rose et al² studied tracking devices for liver ablation procedures using cryogenic ablation (CA), radiofrequency ablation (RFA) and percutaneous ethanol injection (PEI). Conventional 2D ultrasound was used to guide the catheter, needle and ablation probe toward the target. Once the device was thought to be in place, a 3D volume of data was collected to check alignment of the device with the tumor target and the surrounding anatomical structures. The time required for each 3D acquisition, including data manipulation and image interpretation, ranged from 1 to 3 minutes. If the location was deemed undesirable, the ultrasound system was switched back to the 2D mode to reposition the tumor-treating device to a more appropriate location. This new location was then confirmed with 3D ultrasound. Such a process is necessary since the ultrasound system in use was unable to perform real-time 3D scanning. It was reported that images acquired using 3D ultrasound had altered the ablation procedure in almost half of the procedures performed. The repositioning was performed because the 3D helped the physician form a better relationship between internal structures and the interventional device. One issue that arose during the study was a difficulty visualizing the needle tips used during PEI and the RFA, requiring the insertion of stylets or the partial deployment an echogenic device to locate the tip.

Recently, the use of real-time 3D (RT3D) ultrasound imaging has become more widespread in the clinic in the fields of cardiology and obstetrics. The cardiac RT3D system, originally developed at Duke University,^{3,4} has been used to address the inherent limitations associated with conventional 2D imaging techniques such as monoplanar ultrasound. During the past few years, the usefulness of RT3D echocardiography has been demonstrated for the examination of left ventricular function,⁵ detection of perfusion defects,⁶ reduction in scanning times during dobutamine stress echocardiography,⁷ guidance of right ventricle (RV) endomyocardial biopsy,⁸ measurement of peak left ventricle (LV) flow velocities⁹ and evaluation of congenital cardiac abnormalities.¹⁰

In real-time 3D echocardiography, a 2D matrix array transducer is used to steer and focus the ultrasound beam to create a pyramidal volume of data. From the acquired volume, real-time simultaneous B-scan and C-scan views are displayed, in addition to RT3D rendered volumes, 3D pulse-wave Doppler and 3D color flow Doppler.

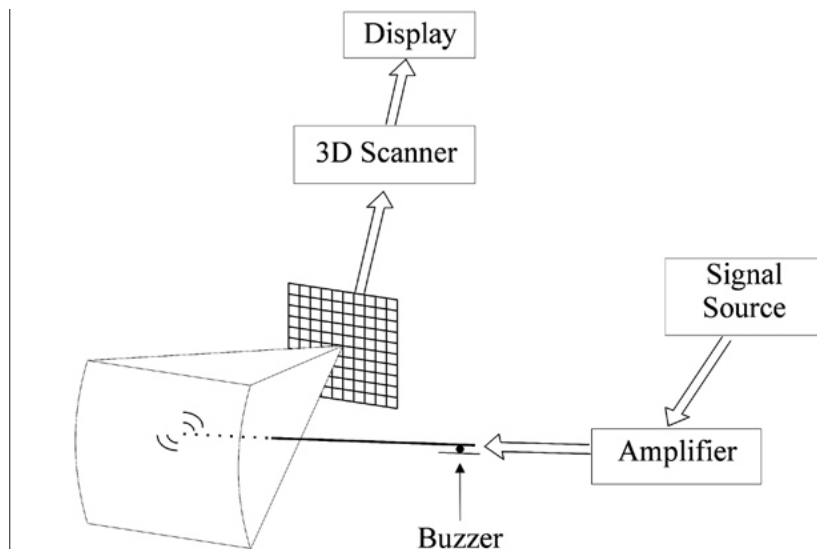


FIG. 1 Schematic of interventional device within 3D beam.

The limitations from the previous studies of guidance of interventional devices show a need for real-time 3D imaging with good tip identification. We hypothesize that attaching piezoelectric actuators to interventional devices will allow real-time device tracking by using 3D color flow Doppler techniques. The advantages of combining real-time 3D ultrasound with the vibrating device techniques could yield superior guidance to current x-ray methods. In this paper, we present 3D tracking experiments both *in vitro* and *in vivo* using a pacemaker lead, Brockenbrough needle for cardiac septal puncture, cardiac guidewire and radiofrequency (rf) ablation needles for cancer therapy. An earlier *in vitro* feasibility study with a single pacemaker stylet was described by Smith et al.¹¹

II. METHODS

Interventional devices

We modified a series of interventional devices by attaching a piezoelectric actuator to couple 1-8 kHz vibrations to each interventional device. The piezoelectric buzzer was driven using a function generator (FG 502) and a 100 W audio amplifier (KLH R3000). Figure 1 shows a schematic of a vibrating interventional device within the pyramidal scan produced by the 2D matrix array transducer.

The first device that we studied is a 2 mm diameter, 73 cm long Biotronik Corox+ LV-H 75 UP coronary sinus pacing lead (Biotronik GmbH & Co., Berlin, Germany) with a buzzer attached to the stylet. The coronary sinus is the preferred site for delivering pacing pulses to the left ventricle. Recently, left ventricular pacing by itself or as part of biventricular pacing techniques has become a more common treatment to treat severe heart failure, intraventricular conduction problems and to reset the sequence or timing of the LV.^{12, 13}

A strain relief mechanism attached to the top of the pacing lead greatly improved the visibility of the tip of the stylet in the image. This mechanism was designed to bear most of the stress associated with the wires, which connect to the piezoelectric actuator that is fixed to the stylet. It enclosed the top of the stylet where the buzzer was located and slid onto the pacing lead when the stylet was inserted into the lumen of the lead. Once the guidance was com-

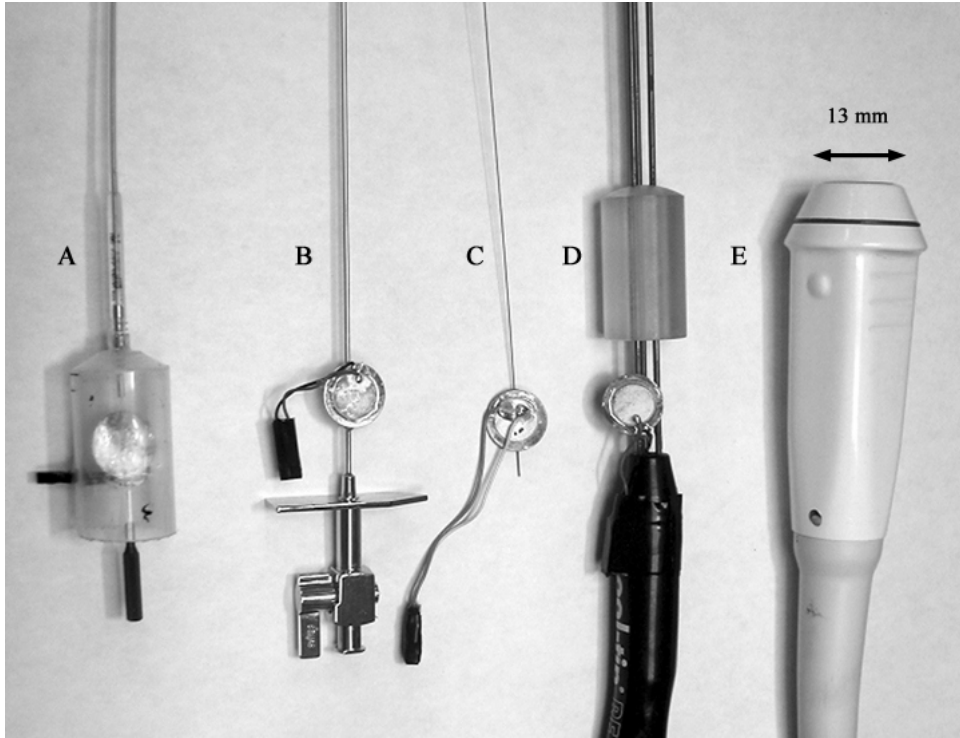


FIG. 2 Photograph of the modified interventional devices and the matrix array. (A) CS pacing lead with strain relief mechanism. (B) Brockenbrough needle used for atrial puncture. (C) Guidewire used for guiding interventional devices. (D) Radiofrequency ablation probe. (E) 2.5 MHz matrix array.

plete, the stylet and the strain relief device could both be removed, permitting permanent lead placement (Fig. 2A).

We also tested the ability to vibrate and track a 1.2 mm diameter, 71 cm long Brockenbrough needle shown in Figure 2B (Daig Corporation, Minnetonka, MN). This needle is introduced into the body via the common femoral vein. It is then tracked up into the right atrium and used to puncture the atrial septum to gain access to the left atrium for radiofrequency ablation.¹⁴

Guidewires are often used to direct other interventional devices to specific locations within the body. Typically, the wire is initially introduced into the site of interest and once in place, an interventional device is slid over them. Such a technique is used to lead a transseptal sheath to the right atrium¹⁴ or to steer over-the-wire pacing leads into the coronary sinus.^{13,15} For our study, we used a 0.36 mm diameter, 85 cm long guidewire with a piezoelectric actuator on the proximal portion (Fig. 2C).

The final interventional device tested was a Cool-tip Cluster Electrode radiofrequency (rf) ablator (Radionics, Tyco Healthcare Group LP, Burlington, Massachusetts) with three 17 gauge, 15 cm long needles that have electrodes at the tip (Fig. 2D). Radiofrequency ablation of hepatic tumors is often employed when a patient cannot be considered for surgery due to the tumor location, insufficient hepatic reserve, excessive tumor burden or other medical conditions that make surgery undesirable.¹⁶

Ultrasound system

The Model 1 ultrasound system (Volumetrics Medical Imaging, Durham, NC) is a commercial version of the real-time volumetric scanner developed at Duke University. The sys-

tem uses up to 512 transmitters and 256 receive channels, and also utilizes 16:1 receive mode parallel receive processing to generate 4096 B-mode image lines at up to 60 volumes per second. The scanner display includes two simultaneous orthogonal B-mode image planes and up to three C-mode planes parallel to the array face. Each image plane can be inclined at any desired angle. By integrating and spatially filtering between two user-selected C-mode planes, the system can display real-time 3D rendered images. Finally, the system offers both spectral Doppler and color flow Doppler features over the complete 3D pyramid.

We modified the system to allow the image planes to be thickened from the standard 0.9 mm up to 9 mm in 0.3 mm increments. The thickened display slices provided the physician with more flexibility by requiring less aligning accuracy to locate the tip of the tool in the display slice. However, the use of thickened slices required more data to be sent to the display, resulting in a decrease in the video frame rate. After the tip is localized, the slice thickness was decreased to increase frame rate during the guidance of the device toward the target.

The color flow Doppler settings for this study included no temporal averaging, data packet sizes of 9, maximum wall filtering, pixel preference set to color over gray scale and a color flow pulse repetition frequency (prf) between 2.4 and 4.5 kHz. The color flow reject setting was adjusted according to the amount of signal present. This helped to limit the visible color signal to only the tip region. The color bar associated with the color flow Doppler was set to show only absolute values from 0 to the maximum shift frequency so that the tip would 'glow' a shade of orange instead of a mixture of blue and red. Using these settings, typical 3D Doppler frame rates ranged from 1.5 to 4 volumes per second during the experiments.

Figure 2E shows the matrix array whose size is typical of standard cardiac probes. This array was used to image the pacing lead, the Brockenbrough needle and the rf ablation needles. A dual lumen forward-looking 22 Fr catheter array transducer equipped with a tool port (Fig. 3) was used to image during the guidewire experiments. This catheter transducer was built and reported by Lee et al.¹⁷

***In vitro* experiments**

The pacing lead and Brockenbrough needle were inserted into a hydraulically beating cardiac ultrasound phantom that is capable of simulating the contraction and filling of the chambers of the heart. While the heart was pumping, interventional devices were inserted into the heart via a port that connected to the right atrium and then were passed into the right ventricle where they were tracked in real-time using the 2.5 MHz transthoracic matrix array and 3D color flow Doppler.

The guide wire was inserted into the tool port of the 22 F catheter array transducer (Fig. 3). In a water tank, the catheter array transducer was then placed above a 4 mm hole in a tissue mimicking sponge. After the piezoelectric buzzer was activated with a driving frequency of 3.4 kHz, the guidewire was advanced into the lumen while being imaged by the transducer using 3D color flow Doppler.

The rf ablation electrodes were imaged within a phantom of excised beef liver. The liver was first soaked overnight in a container of degassed water. The liver was then transferred to a new container of deionized water and held under vacuum for 4 hours to remove air bubbles. After degassing, a balloon 'cyst' was inserted into the center of the liver and used as a target for the experiments. For the experiments, the excised liver was submerged in water with the 2.5 MHz transthoracic matrix array in contact with the upper surface. The rf ablation needles were then inserted into the liver and tracked using real-time 3D color flow Doppler.

Animal model

The *in vivo* images in this study were acquired using a sheep model. The study was approved by the Institutional Animal Care and Use Committee at Duke University and conformed to the Research Animal Use Guidelines of the American Heart Association.

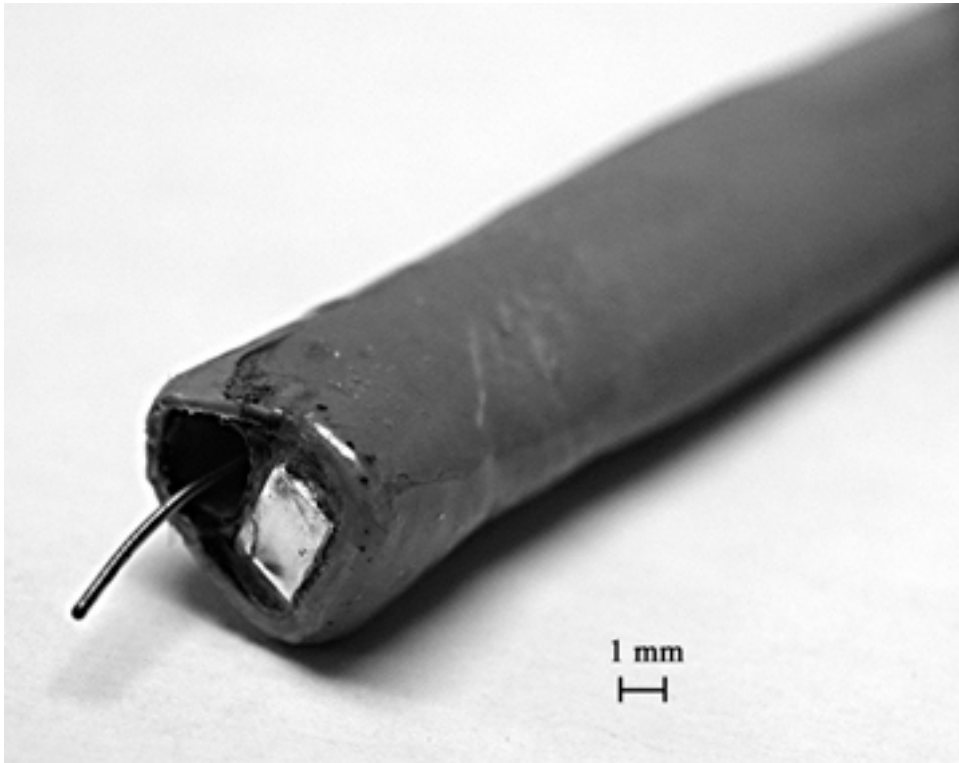


FIG. 3 22 F catheter transducer with guidewire protruding from the tool port of dual lumen catheter.

A total of 15 to 22 mg/kg of intramuscular injected ketamine hydrochloride was used to sedate the animals. A 20 gauge intravenous (IV) catheter was placed in the saphenous vein for the purpose of IV fluid administration and the animal was placed on a water-heated thermal pad. The animals were mechanically ventilated with 95 to 99% oxygen and 1 to 5% isoflurane for anesthesia. A nasogastric tube was passed into the stomach to prevent rumenal typany. A femoral arterial line was placed on the left side *via* a percutaneous puncture, and electrolyte and respirator adjustments were made based on serial electrolyte and arterial blood gas measurements. Sodium chloride (0.9%) was continuously infused as an IV maintenance fluid. Throughout the procedure, blood pressure, lead II ECG and temperature were continuously monitored. For the open chest procedures, the heart was exposed by median sternotomy.

To test our ability to track the pacing lead, four studies were completed using open chest sheep models. The vibrating stylet was inserted into the pacemaker lead, introduced into the jugular vein and advanced to the superior vena cava (SVC) while being scanned with a 2.5 MHz matrix array transducer attached to the Volumetrics system with 3D color flow Doppler. Once the lead was in the right atrium, the sheep's heart was scanned from an epicardial position.

For the liver experiment, one sheep study was performed in a closed model where the gallbladder was targeted using the 2.5 MHz matrix array and the rf ablation probe.

III. RESULTS

In the following figures, arrows to the side of the B-scans define the C-mode planes. Blunt arrows show the relative orientation of the B-scan planes.

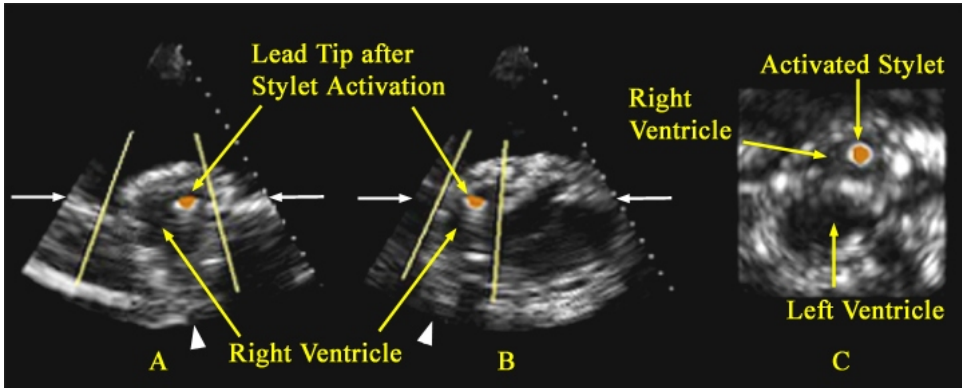


FIG. 4 Images of the pacemaker lead and stylet within the right ventricle of the cardiac phantom. (A) Long axis B-scan of RV. (B) Short axis B-scan of RV. (C) Long axis C-scan of RV.

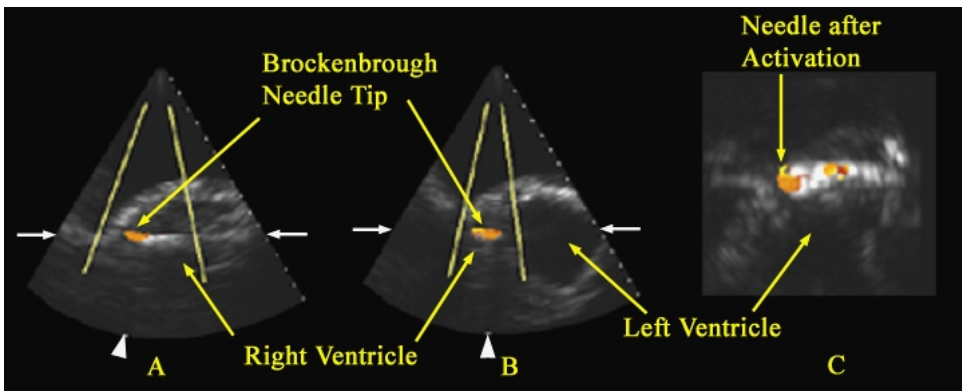


FIG. 5 Brockenbrough needle within the right ventricle of the cardiac phantom. (A) Long axis B-scan. (B) Short axis B-scan. (C) Long axis C-scan image.

***In vitro* studies**

Figure 4 shows the images of a 16 cm deep 3D scan of the pacemaker lead that were all acquired in the cardiac phantom using the 2.5 MHz matrix array. The images show a long axis B-scan view (Fig. 4A), a short axis B-scan (Fig. 4B) and long axis C-scan (Fig. 4C) of the cardiac phantom. An orange dot is clearly visible at the tip of pacing lead where the stylet tip is vibrating inside the lead lumen.

Images of the Brockenbrough needle acquired with the 2.5 MHz matrix array within the cardiac phantom are shown in figure 5. The tip of the needle can be seen in the long axis B-mode image (Fig. 5A), the short axis B-scan image (Fig. 5B) and the long axis C-scan image (Fig. 5C) where vibrations were detected. In this experiment, the vibrating device is not within a sheath, which allowed a stronger Doppler signal to reach the transducer. Therefore, it was necessary to increase the color flow reject level to decrease the amount of color corresponding to the non-tip regions.

Figure 6 shows the images of the guidewire being directed into the lumen in the tissue mimicking sponge, including two long axis B-scan views (Figs. 6A, B) and a cross-sectional C-scan view (Fig. 6C), that were acquired with the 22 F, 5 MHz forward-viewing catheter matrix array. Very strong signals were located at this tip since the transducer distance is

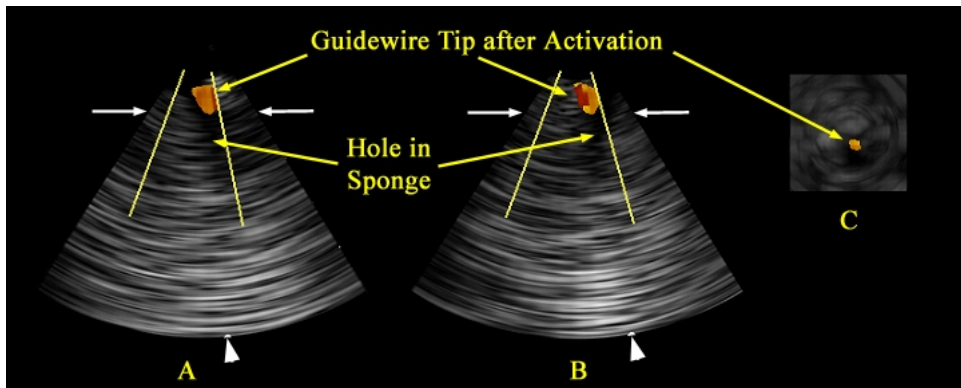


FIG. 6 Catheter transducer images of guidewire within hole of tissue mimicking sponge. (A, B) Long axis B-scan views. (C) Cross-sectional C-scan view.

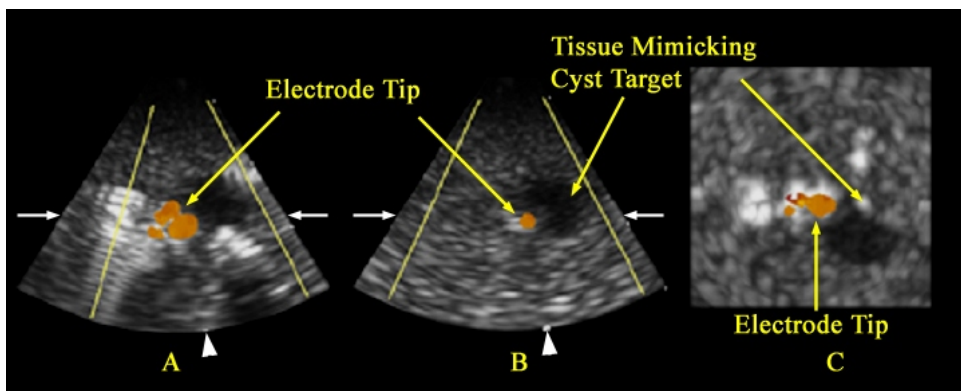


FIG. 7 Rf electrodes needle guided towards 'cyst' in liver phantom. (A) Long axis B-scan view. (B) Short axis B-scan view. (C) Long axis C-scan view.

small and there was little attenuation from the water. For these reasons, the color flow reject was increased to limit the amount of the color displayed at the tip.

Figure 7 shows orthogonal images from a 4 cm deep 3D scan as the rf ablation needles are guided towards the cyst target in the liver phantom. The needles are seen in a long axis B-scan view (Fig. 7A), short axis B-scan view (Fig. 7B) and a long axis C-scan view (Fig. 7C). Probe tracking was possible throughout the entire experiment, although the signal from the tip was weaker while the needles were being advanced.

***In vivo* images**

Figure 8 shows images of a 6 cm 3D scan of the pacing lead within the SVC. In this study, a series of volumes were obtained before the stylet buzzer was activated. Image slices from one of these volumes include a long axis B-scan view (Fig. 8A), a short axis B-scan view (Fig. 8B) and a long axis C-scan view (Fig. 8C). In the B-scan images, it is difficult to differentiate the pacing lead from the surrounding vessel lumen while a bright echo from the lead can be visualized in the long axis C-scan view. After the buzzer was activated with a driving frequency of 3.3 kHz, images from another 3D scan were displayed, including a long axis B-scan view (Fig. 8D), a short axis B-scan (Fig. 8E) and a long axis C-scan (Fig. 8F). In this second set, the pacing lead tip is seen lying along the vessel wall and can be distinguished

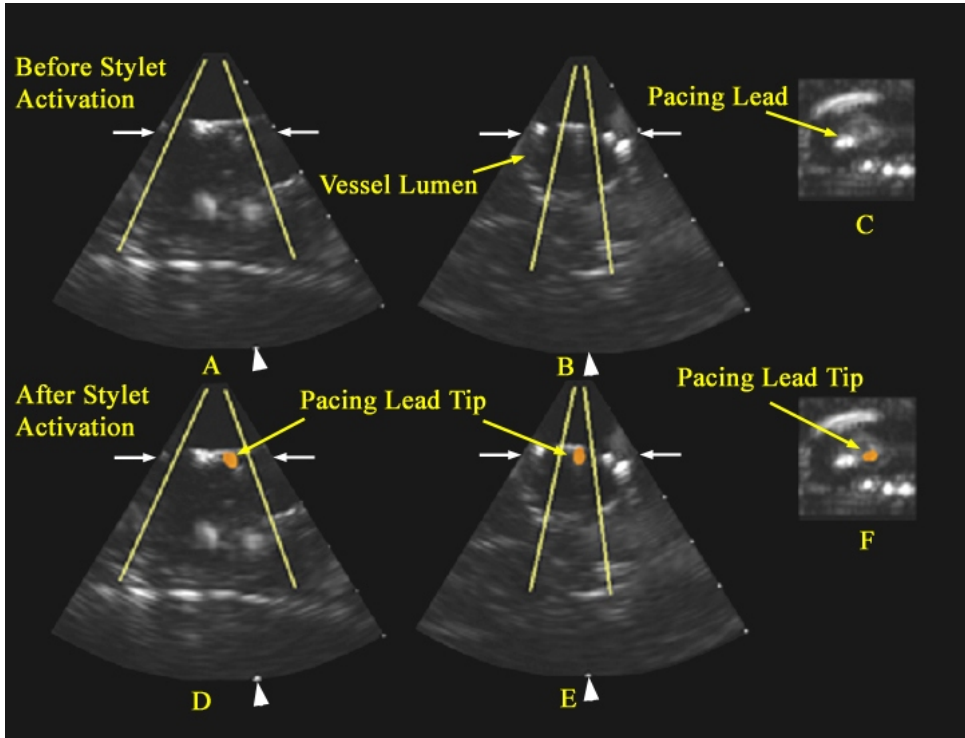


FIG. 8 Pacemaker lead visualized within the SVC. *Before stilet activation*: (A) Long axis B-scan view. (B) Short axis B-scan. (C) Long axis C-scan. *After stilet activation*: Orange dot indicated tip location. (D) Long axis B-scan view. (E) Short axis B-scan. (F) Long axis C-scan.

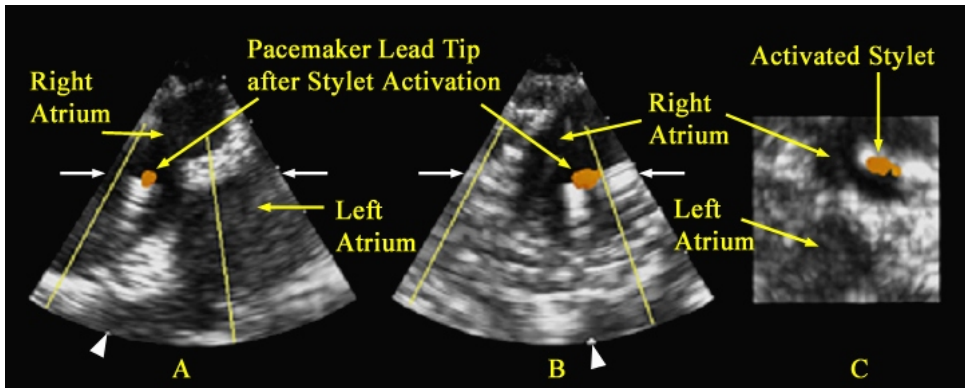


FIG. 9 Epicardial view of RA containing the pacing lead. (A, B) Long axis B-scans. (C) Short axis C-scan.

from the surrounding soft tissue in all three views. When comparing the C-scans before and after activation, one can see that the true location of the lead tip in figure 8F was not indicated by the echo in figure 8C.

Figure 9 shows images from a 6 cm epicardial scan of the pacemaker lead in the right atrium obtained by the 2.5-MHz matrix array transducer, including two long axis B-scans (Figs. 9A, B) and a short axis C-scan (Fig. 9C). Again a large orange dot indicates the tip location in all three views once the stilet was activated.

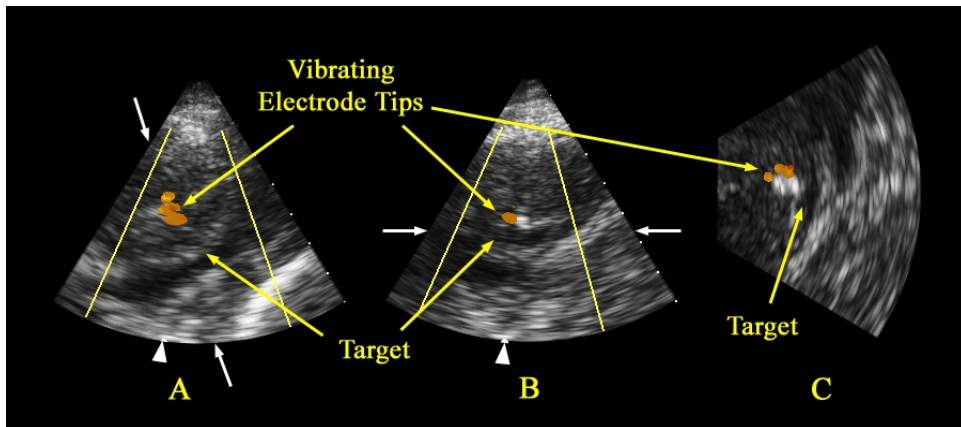


FIG. 10 Tracking the rf electrodes toward gallbladder target in a closed animal model. (A, B) Oblique B-scan. (C) Oblique C-scan.

Images from an 8 cm 3D liver scan acquired with the 2.5 MHz matrix array in the intact sheep model are shown in figure 10. The rf ablation electrodes can be identified by the orange dot in oblique B-scan views (Figs. 10A, B) as well as an oblique C-scan view (Fig. 10B) as they are guided toward the gallbladder target. Some of the signal was lost while advancing the device when the needles are cutting tissue, which results in a damping of the tip vibrations.

IV. DISCUSSION

The objective of this study was to see if real-time 3D color flow Doppler improved tracking of interventional devices. Despite some limitations, it seems that the advantages of real-time 3D ultrasound along with the ability to reliably visualize the device tip provide the operator with new information that should help increase the confidence level of guiding such tools.

In our study, real-time 3D ultrasound guidance improved the ability to visualize and track interventional devices, especially in the case of the radiofrequency ablation needles. Our system has the ability to acquire 3D pyramidal volumes in real-time, including color flow Doppler data, which allows us to track the interventional devices in 3D at all times. The addition of the piezoelectric buzzer aided in our ability to distinguish the tip from the surrounding tissue when combined with 3D color flow Doppler.

There are some limitations that must be addressed. We must consider reducing the size of the 22 F catheter transducer to make it more feasible for clinical application. Also, the reduced spatial resolution associated with our images, when compared to those of standard 2D ultrasound systems, may limit the success of tracking. We could try to minimize this effect by using high frequency transducers but this would decrease our depth penetration.

We were unable to track the pacemaker lead once it entered the right ventricle due to artifacts from ventricular wall motion in this region. It may be possible to limit the artifacts in the RV by narrowing the Doppler filter bandwidth and only passing the frequency range corresponding to the stylet tip. Pacing lead tracking was also less successful when the lead was bent, possibly because the stylet vibrations were damped by the lead lumen and unable to reach the tip. These two findings may limit the effectiveness of guiding pacing leads using our current methods.

The artifact described during the *in vivo* pacing lead study was not an issue during the rf ablation needle tracking. The rigid nature of the device allowed vibrations to travel down the length of the needles to the tip. Also, the background noise level was lower since the blood flow velocities are much lower in the hepatic and portal veins than the vibrating tip velocity.

During the animal studies, the limited frame rate associated with the color flow Doppler mode on the ultrasound system required the devices to be guided in an unusually slow manner. This effect was magnified when the color flow Doppler gates were widened or when the image planes were thickened, when only 1.5 3D Doppler volumes were displayed per second. One solution may be to decrease the packet size over which the Doppler shift is calculated, but at the expense of Doppler signal-to-noise ratio.

ACKNOWLEDGMENTS

The authors thank Edward D. Light and Ellen Dixon-Tulloch for their assistance on this project. We also thank Critical Care Innovations for providing the buzzers and Biotronik for the pacing lead. This project supported in part by NIH grants HL64962 and HL72840.

REFERENCES

1. Armstrong G, Cardon L, Vilkomerson D, et al. Localization of needle tip with color Doppler during pericardiocentesis: in vitro validation and initial clinical application, *J Amer Soc Echocardiog* 14, 29-37 (2001).
2. Rose SC, Hassanein TI, Easter DW, et al. Value of three-dimensional US for optimizing guidance for ablating focal liver tumors, *J Vasc Intervent Radiol* 12, 507-515 (2001).
3. Smith SW, Pavy HG, von Ramm OT. High-speed ultrasound volumetric imaging-system: 1. transducer design and beam steering, *IEEE Trans Ultrason Ferroelect Freq Contr* 38, 100-108 (1991).
4. von Ramm OT, Smith SW, Pavy HG. High-speed ultrasound volumetric imaging-system: 2. parallel processing and image display, *IEEE Trans Ultrason Ferroelect Freq Contr* 38, 109-115 (1991).
5. Schmidt MA, Ohazama CJ, Agyeman KO, et al. Real-time three-dimensional echocardiography for measurement of left ventricular volumes, *Amer J Cardiol* 84, 1434-1439 (1999).
6. Camarano G, Jones M, Freidlin RZ, Panza JA. Quantitative assessment of left ventricular perfusion defects using real-time three-dimensional myocardial contrast echocardiography, *J Amer Soc Echocardiog* 15, 206-213 (2002).
7. Ahmad M, Xie TR, McCulloch M, et al. Real-time three-dimensional dobutamine stress echocardiography in assessment of ischemia: comparison with two-dimensional dobutamine stress echocardiography, *J Amer Coll Cardiol* 37, 1303-1309 (2001).
8. McCreery CJ, McCulloch M, Ahmad M, deFilippi CR. Real-time 3-dimensional echocardiography imaging for right ventricular endomyocardial biopsy: a comparison with fluoroscopy, *J Amer Soc Echocardiog* 14, 927-933 (2001).
9. Tsujino H, Jones M, Shiota T, et al. Real-time three-dimensional color Doppler echocardiography for characterizing the spatial velocity distribution and quantifying the peak flow rate in the left ventricular outflow tract, *Ultrasound Med Biol* 27, 69-74 (2001).
10. Fleishman CE, Li J, Ota T, et al. Identification of congenital heart defects using real time three-dimensional echo in pediatric patients, *Circulation* 94, 2423-2423 (1996).
11. Smith SW, Booi RC, Light ED, et al. Guidance of cardiac pacemaker leads using real time 3D ultrasound: Feasibility studies, *Ultrasonic Imaging* 24, 119-128 (2002).
12. Bashir JG, Tyers GFO, Lampa M, Yamaoka R. Combined use of transesophageal echo and fluoroscopy for the placement of left ventricular pacing leads via the coronary sinus, *Pace-Pacing Clin Electrophysiol* 26, 1951-1954 (2003).
13. Artrip JH, Sukerman D, Dickstein ML, Spotnitz HM. Transesophageal echocardiography guided placement of a coronary sinus pacing lead, *Ann Thoracic Surg* 74, 1254-1256 (2002).

14. Lesh MD, Guerra PG, Roithinger FX, et al. Novel catheter technology for ablative cure of atrial fibrillation, *J Intervent Card Electrophysiol* 4, 127-139 (2000).
15. Blanc JJ, Etienne Y, Gilard M, et al. Evaluation of different ventricular pacing sites in patients with severe heart failure – results of an acute hemodynamic study, *Circulation* 96, 3273-3277 (1997).
16. Montgomery RS, Rahal A, Dodd GD, et al. Radiofrequency ablation of hepatic tumors: Variability of lesion size using a single ablation device, *Amer J Roentgen* 182, 657-661 (2004).
17. Lee W, Idriss SF, Wolf PD, Smith SW. Dual lumen transducer probes for real-time 3-D interventional cardiac ultrasound, *Ultrasound Med Biol* 29, 1297-1304 (2003).
18. Smith SW, Lopath PD, Adams DB, Walcott GP. Cardiac ultrasound phantom using a porcine heart model, *Ultrasound Med Biol* 21, 693-697 (1995).